12 *Chem. Mater.* **2010,** *22,* 12–14
DOI:10.1021/cm902239a

CHEMISTRY OF MATERIALS
Communication

Mesoporous Silica Nanoparticles with Remarkable Stability and Dispersibility for Antireflective Coatings

Yasuto Hoshikawa,[†] Hiroki Yabe,[‡] Atsuro Nomura,[†] Takeyuki Yamaki,[‡] Atsushi Shimojima,[†] and Tatsuya Okubo*,[†]

[†]*Department of Chemical System Engineering, the University of Tokyo, 7-3-1 Hongo, Bunkyo-ku, Tokyo 113-8656, Japan and* [‡]*Advanced Technologies Development Laboratory, Panasonic Electric Works Co., Ltd., 1048 Kadoma, Osaka 571-8686, Japan*

Received July 22, 2009
Revised Manuscript Received November 16, 2009

Mesoporous silica synthesized via the surfactant-templating route is currently attracting significant interest as a low dielectric constant (low-*k*) and low refractive index (low-*n*) materials, because of its high porosity and high thermal and mechanical stability.[1] Highly ordered mesoporous silica films have been prepared by evaporation induced self-assembly (EISA) processes,[2] and excellent dielectric properties and an ultralow refractive index have been reported.[2−4] However, there are several drawbacks that make practical applications difficult. The EISA process generally requires precise control over the experimental conditions. Additionally, post calcination process at high-temperature for surfactant removal is undesirable, especially when the films are coated on thermally unstable polymer substrates. One promising approach to address these issues is the use of well-dispersed mesoporous silica nanoparticles (MSNs) embedded in silica or other polymer matrices to produce nanocomposite films. The following advantages are expected: (i) the synthesis of mesoporous silica including surfactant removal can be separated from the coating process; (ii) various matrix polymers, either organic or inorganic, are available; and (iii) closed mesopores can be formed when nonporous matrix is employed. We have focused on the application of such nanocomposite materials as low-*n* films, which are practically important for high-performance antireflective (AR) coatings used in optical display devices.

Previously, various MSNs with controlled diameters, shapes, pore architectures, and colloidal dispersibility[5] have been synthesized and examined for various applications.[6] However, the low-*n* applications based on MSNs have been very limited.[5g] For these applications, removal of the surfactants from the mesostructured silica−surfactant composite nanoparticles (SSNs) is required, without the loss of monodispersity and the internal mesostructure. Modification of the internal and external surfaces of nanoparticles with organic groups is also important for stabilization of the mesostructure, to create hydrophobic pores to minimize water adsorption,[3] and to control the interface between the particle surface and the matrix polymer.

Here we report the preparation of a stable dispersion of organically modified MSNs in alcohols by simultaneous trimethylsilylation and surfactant extraction, and we demonstrate that these nanoparticles can be used for the fabrication of nanocomposite films with well-dispersed nanoparticles in a silica matrix. These films have remarkable AR properties that are enhanced by increasing the pore volume of the MSNs with swelling agents during synthesis.

Mesostructured SSNs were prepared from a mixture of tetraethoxysilane (TEOS), 3-aminopropyltriethoxysilane (APTES), cetyltrimethylammonium bromide (CTAB), water, ethylene glycol (EG) by stirring at 333 K for 4 h.[6b] The molar composition of the reactants was 1.00:0.16:1.06:25.6:104:2150 TEOS:APTES:CTAB:NH_3:EG:H_2O. To enhance the porosity of the nanoparticles, 1,3,5-trimethylbenzene (TMB)[7] was added as a swelling agent to this mixture at the beginning of the reaction. Three samples were prepared with molar ratios of TMB/CTAB = 0, 2, and 4.

To achieve direct trimethylsilylation of SSNs in an aqueous dispersion, we have developed a new process based on the modified Lentz method, where hexamethyldisiloxane (HMDS) is used as the silylation agent under highly acidic conditions.[8] The reaction was performed by adding as-synthesized dispersions of SSNs to a mixture of HMDS, 2-propanol, water, and HCl, followed by stirring the biphasic mixture at 345 K.[9] Under these conditions,

*Corresponding author. E-mail: okubo@chemsys.t.u-tokyo.ac.jp. Phone: +81-3-5841-7348. Fax: +81-3-5800-3806.

(1) Schüth, F.; Schmidt, W. *Adv. Mater.* **2002**, *14*, 629–638.
(2) (a) Zhao, D.; Yang, P.; Melosh, N.; Feng, J.; Chmelka, B. F.; Stucky, G. D. *Adv. Mater.* **1998**, *10*, 1380–1385. (b) Lu, Y.; Fan, H.; Doke, N.; Loy, D. A.; Assink, R. A.; LaVan, D. A.; Brinker, C. J. *J. Am. Chem. Soc.* **2000**, *122*, 5258–5261.
(3) Baskaran, S.; Liu, J.; Domansky, K.; Kohler, N.; Li, X.; Coyle, C.; Fryxell, G. E.; Thevuthasan, S.; Williford, R. E. *Adv. Mater.* **2000**, *12*, 291–294.
(4) Konjhodzic, D.; Schroter, S.; Marlow, F. *Phys. Status Solidi* **2007**, *11*, 3676–3688.
(5) (a) Nooney, R. I.; Thirunavukkarasu, D.; Chen, Y.; Josephs, R.; Ostafin, A. E. *Chem. Mater.* **2002**, *14*, 4721–4728. (b) Suzuki, K.; Ikari, K.; Imai, H. *J. Am. Chem. Soc.* **2004**, *126*, 462–463. (c) Urata, C.; Aoyama, Y.; Tonegawa, A.; Yamauchi, Y.; Kuroda, K. *Chem. Commun.* **2009**, 5094–5096. (d) Sadasivan, S.; Khushalani, D.; Mann, S. *J. Mater. Chem.* **2003**, *13*, 1023–1029. (e) Han, Y.; Ying, J. Y. *Angew. Chem., Int. Ed.* **2005**, *44*, 288–292. (f) Moller, K.; Kobler, J.; Bein, T. *Adv. Funct. Mater.* **2007**, *17*, 605–612. (g) Kobler, J.; Bein, T. *ACS Nano* **2008**, *2*, 2324–2330.
(6) (a) Slowing, I. I.; Trewyn, B. G.; Giri, S.; Lin, V. S.-Y. *Adv. Funct. Mater.* **2007**, *17*, 1225–1236. (b) Gu, J.; Fan, W.; Shimojima, A.; Okubo, T. *Small* **2007**, *10*, 1740–1744. (c) Liu, J.; Stace-Naughton, A.; Jiang, X.; Brinker, C. J. *J. Am. Chem. Soc.* **2009**, *131*, 1354–1355. (d) Huang, Y.; Trewyn, B. G.; Chen, H.-T.; Lin, V. S.-Y. *New J. Chem.* **2008**, *32*, 1311–1313.
(7) Beck, J. S.; Vartuli, J. C.; Roth, W. J.; Leonowicz, M. E.; Kresge, C. T.; Schmitt, K. D.; Chu, C. T-W.; Olson, D. H.; Sheppard, E. W.; McCullen, S. B.; Higgins, J. B.; Schlenker, J. L. *J. Am. Chem. Soc.* **1992**, *114*, 10834–10843.
(8) Lentz, C. W. *Inorg. Chem.* **1964**, *3*, 574–579.
(9) see the Supporting Information for details.

 Published on Web 12/01/2009

cleavage of HMDS and exchange of the surfactant cations with protons proceed, resulting in trimethylsilylation of the silanol groups on both the internal and external surfaces of SSNs. Trimethylsilylated (TMS)-MSNs were easily separated from the oil phase by centrifugation.

X-ray diffraction (XRD) pattern of TMS-MSNs prepared without TMB shows four diffraction peaks, indexed as (10), (11), (20) and (21) reflections of a two-dimensional (2D) hexagonal (*p6mm*) structure with a d_{10} spacing of 3.9 nm (see Figure S1 in the Supporting Information).[9] The d_{10} spacing is increased to 5.0 and 5.9 nm by the addition of TMB at the TMB/CTAB ratios of 2.0 and 4.0, respectively, which suggests that TMB acts as a swelling agent to increase the diameter of the cylindrical assemblies in this system.

Solid-state ^{29}Si MAS NMR spectrum of TMS-MSNs prepared without TMB shows five signals; Q^2, Q^3, and Q^4 signals (Q^n: $Si(OSi)_n(OH \text{ or } O^-)_{4-n}$), a T^3 ($CSi(OSi)_3$) signal due to aminopropylsilyl groups, and a M^1 signal due to trimethylsilyl groups ($\equiv SiOSiMe_3$) (see Figure S2 in the Supporting Information).[6b] The presence of trimethylsilyl groups was also confirmed by ^{13}C cross-polarization (CP)/MAS NMR (see Figure S3 in the Supporting Information).[9] In addition, ^{13}C CP/MAS NMR and FT-IR analyses confirmed that the surfactants were completely removed (see Figure S4 in the Supporting Information).[9] From the ^{25}Si MAS NMR data, the integral intensity ratio of $M^1/(M^1 + T^3 + Q^n)$ is 0.15, which is much higher than the theoretical ratio of SiOH groups on the external surface of the nanoparticles (ca. 0.02).[9] These results suggest that trimethylsilyl groups ($-OSiMe_3$) are attached to both the internal and external surfaces of MSNs via Si−O−Si bonds.

Field-emission scanning electron microscopic (FE-SEM) images of TMS-MSNs are shown in Figure 1(left). The particle sizes are in the range of 40−80 nm and are almost unchanged by the addition of TMB. Transmission electron microscopic (TEM) images (Figure 1(right)) show discrete spherical particles with either well-ordered hexagonal dot patterns or striped patterns. The increase in pore diameter by the addition of TMB is also evident. When TMB/CTAB = 4, the cylindrical pores become more enlarged but less-ordered near the particle surface, and irregular open pores on the particles can be observed by SEM.

The nitrogen adsorption−desorption measurements revealed the highly porous nature of TMS-MSNs (see Figure S5 in the Supporting Information).[9] The Brunauer−Emmett−Teller (BET) surface areas, average pore diameters evaluated by Barrett−Joyner−Halenda (BJH) method, pore volumes, and wall thicknesses calculated from the pore diameters and the d_{10} spacings are summarized in Table 1. The addition of TMB caused a significant increase in pore diameter, whereas the wall thickness remained almost unchanged; therefore, the total pore volume of TMS-MSNs was increased.

TMS-MSNs have excellent dispersibility in such alcohols as ethanol, 2-propanol, butanol, and hexanol, as

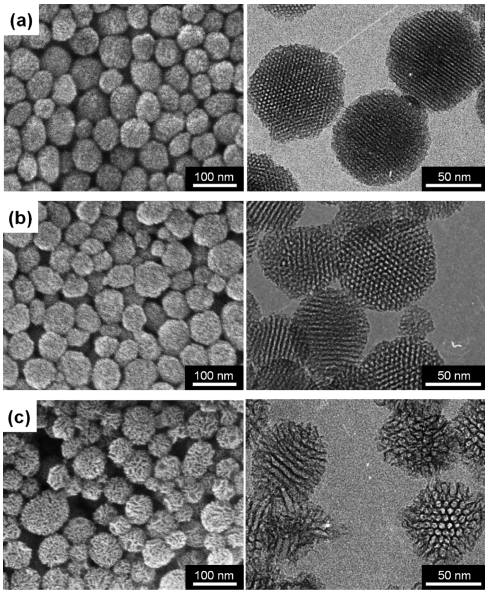

Figure 1. (left) FE-SEM and (right) TEM images of TMS-MSNs prepared with TMB/CTAB ratios of (a) 0, (b) 2, and (c) 4.

Table 1. Structural Parameters of TMS-MSNs

TMB/CTAB ratio	d_{10} spacing (nm)	BJH Pore diameter (nm)	wall thickness (nm)	BET surface area ($m^2\ g^{-1}$)	pore volume ($cm^3\ g^{-1}$)
0	3.9	2.5	2.1	943	1.3
2	5.0	3.7	2.3	857	1.5
4	5.9	5.0	2.0	829	1.9

confirmed by dynamic light scattering (DLS) measurements (see Figure S6 in the Supporting Information).[9] A dispersion of TMS-MSNs in 2-propanol can be concentrated up to 8 wt % and no precipitation or structural deterioration were observed, even after one month. It should be noted that when the surfactant was removed from SSNs by conventional acid (HCl) treatment in ethanol, particle aggregation and partial deterioration of the mesostructure occurred (see Figures S6 and S7 in the Supporting Information).[9] The lower dispersibility of such unsilylated MSNs compared to TMS-MSNs was pronounced when the dried samples were redispersed in 2-propanol.[9] Furthermore, these unsilylated MSNs gradually underwent structural collapse under ambient conditions.[9] Therefore, it is plausible that the trimethylsilyl groups in TMS-MSNs play a crucial role in preventing the rearrangement of the siloxane networks and irreversible aggregation of the nanoparticles caused by the formation of Si−O−Si bonds between particles.

The characteristic properties of TMS-MSNs are desirable for the fabrication of nanocomposite films for low-*n* applications. The nanocomposite films were prepared by coating the mixture of TMS-MSNs and siloxane oligomers,[9] and their potential for use as an AR coating was tested. It appeared that the film containing 30 wt % TMS-MSNs had enough mechanical strength for practical use. SEM observations (Figure 2a) show that the thickness of the film is 100−120 nm and that the nanoparticles are uniformly embedded in the silica matrix. From atomic force microscopy (AFM) mapping of the

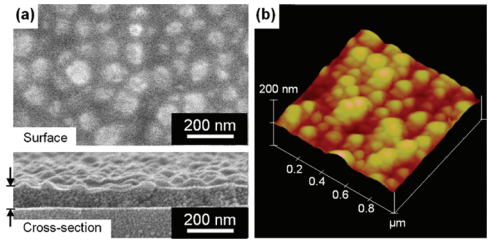

Figure 2. (a) FE-SEM images of the surface and the cross-section of a nanocomposite film containing 30 wt % TMS-MSNs prepared without TMB, and (b) an AFM image of the surface.

surface (Figure 2b), the average roughness is estimated to be ca. 2.5 nm, which is sufficiently small to ensure high optical transparency.

The reflected light from the air−film interface is generally represented by the reflection coefficient $r = (n_2 - n_1)/(n_2 + n_1)$, where n_1 and n_2 are the refractive indices of air and film, respectively.[10] The reflection coefficient R, can be represented by the energy of reflected light as follows: $R = |r|^2$. It is therefore expected that the incorporation of TMS-MSNs into a silica film leads to a decrease in the R value. In addition, the AR properties of single-layer films depend on the destructive interference of the reflected light wave under the following conditions: $d = \lambda/4n_2$, where d is the film thickness, and λ is wavelength of visible light. Because human eyes are the most sensitive to light in the wavelength of 550 nm,[11] a suitable thickness for the film is estimated to be 95−125 nm when the n_2 value is in the range of 1.45−1.10. Such a composite film has suitable thickness for AR coating, which is due to the small particle size.

Figure 3 shows a comparison of visible-light reflectivity for a glass substrate, silica film, and nanocomposite films containing 30 wt % TMS-MSNs with different pore volumes. The reflection curves for the silica and composite films have minimum values in the wavelength region of 400−600 nm. Importantly, the nanocomposite films exhibit lower reflectivity than that for the silica film. The minimal reflectivities for these films (1.5−2.5%) tentatively meet the requiement for AR coatings on a glass substrate. The relative reflectivity decreases with the increasing pore size and content of TMS-MSNs loaded in the silica matrix (see Figure S8 in the Supporting Information).[9] From these results, it is evident that the decrease in reflectivity is attributable to the decrease in the refractive index of the film, because of the highly porous MSNs well-dispersed in the films. Also noted is that the penetration of the matrix polymers into the mesopores is substantially negligible in this system.

As another candidate for porous fillers, hollow silica spheres can be used for preparing AR coating.[12] Typical hollow silica spheres of 50−100 nm in diameter have the

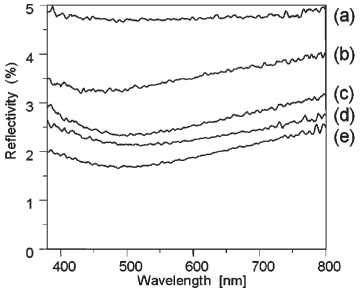

Figure 3. Relationships between reflectivity and the wavelength of visible light for (a) a glass substrate, (b) silica film derived from MS51, and nanocomposite films containing 30 wt % of TMS-MSNs prepared at TMB/CTAB ratios of (c) 0, (d) 2, and (e) 4.

shell thickness of 7.5−20 nm.[13] The calculated porosity of a hollow silica sphere (assuming the diameter of 80 nm and the shell thickness of 10 nm) is ca. 42%, which is still lower than the value (ca. 48%) for TMS-MSNs prepared with TMB/CTAB = 4 (pore size of 5 nm and the wall thickness of 2 nm). Thus the nanocomposite films prepared with MSNs should exhibit better antireflective performance. The ease in controlling the particle size while keeping the same porosity is also a great advantage of MSNs. Furthermore, we expect that MSNs have higher mechanical strength because of its honeycomb structure. Detailed comparison will be made in near future.

In conclusion, the synthesis of MSNs with high stability and dispersibility suitable for thin film application was achieved. Trimethylsilylation was effective, not only for the removal of surfactant while retaining highly ordered mesostructures but also for the long-term stability of the dispersion in alcohol and the internal mesostructure. The nanoparticle dispersions were used for fabrication of nanocomposite films with excellent AR properties. Efforts are underway to further enhance the performance of the composite film based on precise tuning of the particle size, porosity, and the loading amount of mesoporous silica nanoparticles in the matrix.

Acknowledgment. This work was supported in part by Panasonic Electric Works Co., Ltd. The authors are grateful to Dr. A. Fukuoka (The University of Tokyo) for helpful discussions. Y.H. acknowledges the partial support from a Grant-in-Aid for Young Scientists (B) (21760527) from MEXT, Japan. T.O. acknowledges the partial support from a Grant-in-Aid for Scientific Research (B) (No. 20360355) from JSPS, Japan. TEM observations were conducted at the Center for Nano Lithography & Analysis, the University of Tokyo, supported by MEXT.

Supporting Information Available: Experimental details and Figures S1−S8 (PDF). This material is available free of charge via the Internet at http://pubs.acs.org.

(10) Chen, D. *Sol. Energy Mater. Sol. Cells* **2001**, *68*, 313–336.
(11) Ohishi, T.; Maekawa, S.; Ishikawa, T.; Kamoto, D. *J. Sol−Gel Sci. Technol.* **1997**, *8*, 511–515.
(12) Ohata, K.; Yoshihara, T. Japan Patent P2002−265866A, **2002**.
(13) (a) Chen, Y.; Kang, E-T; Neoh, K.-G.; Greiner, A. *Adv. Funct. Mater.* **2005**, *15*, 113–117. (b) Fuji, M.; Takai, C.; Tarutani, Y.; Takei, T.; Takahashi, M. *Adv. Powder Technol.* **2007**, *18*, 81–91. (c) Ma, H.; Zhou, J.; Caruntu, D.; Yu, M. H.; Chen, J. F.; O'Connor, J.; Zhou, W. L. *J. Appl. Phys.* **2008**, *103*, 07A320.